FEATURE ARTICLE

Resonances: Bridge between Spectroscopy and Dynamics

Joel M. Bowman

Department of Chemistry and Cherry L. Emerson Center, Emory University, Atlanta, Georgia 30322

Received: January 8, 1998; In Final Form: March 4, 1998

Resonances are metastable, quasibound states of a molecular complex. They are formed predominantly by vibrational excitation of a molecular complex above a dissociation threshold. Resonances share a number of features in common with bound states, including the possibility of making spectroscopic assignments of them. Thus, resonances can be viewed as the bridge between the bound state spectrum, conventionally the domain of spectroscopy, and the continuum, which is the domain of dynamics. I review a variety of methods from a number of articles to calculate and characterize resonances, with a special focus on resonances in HCO, which have been extensively studied both theoretically and experimentally. HCO represents an extreme case, where most resonances are isolated and nonoverlapping. The effect of overall rotation on resonance positions and widths of HCO is examined in detail, and I present tests of several approximate treatments of rotation. I also point out the role that resonances play in the dynamics of unimolecular reactions, radical−radical reactions, and recombination/dissociation reactions, again using HCO as the key example. The use of "reduced dimensionality" ideas to obtain full dimensional reaction probabilities for a resonance-dominated reaction is illustrated for the OH + CO → H + CO_2 reaction, with special attention to the role of the "spectator" CO-stretch.

I. Introduction

Dynamical resonances in gas-phase or gas-surface collisions refer to long-lived, metastable states of association of molecular fragments (or a molecule with a surface). These states are also referred to as quasibound states, metastable states, and bound states in the continuum. The theoretical and experimental study of resonances has grown enormously in the past decade. There are two broad areas in gas-phase dynamics where resonances play a prominent role. One is in photodetachment spectroscopy, applied to transition state resonances. In this work a neutral, *unbound*, reactive system is created near the saddle point of the reaction by detachment of an electron from the corresponding, *bound* anion. Theoretical and experimental work in this field up to 1990 has been reviewed by Schatz,[1] and Manolopoulos[2] has given a very recent review of the field, with emphasis on the beautiful comparisons between theory and experiment on FH_2^-. (Note, not all structure in photodetachment experiments correspond to resonances.)

The second area where resonances play a primary role, the subject of this article, is the dynamics of systems supported by wells (e.g., radical−radical systems). For this class of systems, the wells support bound states as well as resonances, and it is natural to view resonances as the continuation of the bound-state spectrum into the continuum. In this sense, resonances are a bridge between spectroscopy and dynamics.

Resonances have been calculated and characterized for a small number of important radical−radical systems. These include the simple dissociation reaction HCO → H + CO, about which much more will given below, HO_2 → H + O_2, OH + O,[3−12] H_3^+,[13] LiHF,[14−17] the four-atom system HOCO → OH + CO, H + CO_2, in two,[18−20] three,[21,22] four,[23] and five[24] degrees of freedom, a reduced dimensionality calculation of resonances in ketene isomerization,[25] and statistical calculations of resonances in H_2CO, which have been measured experimentally.[26]

The scope of this article must necessarily be limited, and so I focus on two case studies for which there is extensive theoretical and experimental work: HCO and HOCO. In the next section, which is devoted to calculations on HCO, I describe the various theoretical methods that have been used to calculate and characterize resonances. The first set of calculations and comparisons with experiment are for nonrotating HCO. Then I consider very recent calculations for rotating HCO, using approximate and exact methods. Following that, I review the role of resonances in kinetic theories of recombination, and present results of calculations. This section concludes with a brief review of scattering calculations of dissociation of HCO in collisions with Ar. The role of resonances in the H + CO_2 → [HOCO] → OH + CO reaction is reviewed in section 3, with an emphasis on the reduced dimensionality treatment of reactions that proceed via complex formation. A summary and some remarks about possible future directions are given in section 4.

2. Resonances in HCO

Methods and Calculations. Calculations of resonances in HCO were first done in 1986.[27,28] These and later calculations[29,30] were done using the coupled-channel scattering method for zero total angular momentum. The potential used was a Legendre polynomial representation[31] of a global potential surface based on ab initio calculations.[32]

S1089-5639(98)00725-7 CCC: $15.00
Published on Web 04/15/1998

Resonances were found and characterized using the Smith collision lifetime matrix **Q**,[33] which is given by

$$\mathbf{Q}(E) = i\hbar\mathbf{S}(E)\frac{d\mathbf{S}^{\dagger}(E)}{dE} \quad (1)$$

where E is the total energy and **S** is the scattering matrix. In the vicinity of a resonance **Q**(E) displays a sharp increase, and for isolated resonances, Tr**Q**(E) has a Lorentzian form, which can be fit to obtain the precise values of the resonance positions and widths. So-called partial widths, which contain information about the decay of a resonance into asymptotic internal states of the fragments, can also been obtained from the diagonal elements of **Q**(E).

The Lorentzian form of Tr**Q**(E) follows from the mathematical definition of a resonance as a first-order pole of the scattering matrix in the complex energy plane. Thus, for an isolated (narrow) resonance, an element of the scattering matrix is given by

$$S_{j\rightarrow j'} = \frac{A_{j\rightarrow j'}}{E - \tilde{E}_k}; \quad \tilde{E}_k = E_k - i\frac{\Gamma_k}{2} \quad (2)$$

where E_k and Γ_k are the position and width of resonance, respectively, and j and j' represent initial and final quantum states. Given this mathematical definition of a resonance, it immediately follows that the associated transition probability $P_{j\rightarrow j'}(E)$, which is simply $|S_{j\rightarrow j'}(E)|^2$, is given by

$$P_{j\rightarrow j'}(E) = \frac{|A_{j\rightarrow j'}|^2}{(E - E_k)^2 + \left(\frac{\Gamma_k}{2}\right)^2} \quad (3)$$

which is a Lorentzian function. For this to be actually realized in a given problem two conditions must be satisfied. First, the resonance has to be isolated (i.e., adjacent resonances should not overlap), and second, the resonance has to be narrow (i.e., the so-called background contribution to the scattering has to be constant over the width of the resonance).

The method to extract resonance information from scattering calculations by fitting Tr**Q** or scattering probabilities to Lorentzian forms had been by far the most widespread approach prior to 1995. It was used in the early work of Bowman and Wagner and co-workers to characterize resonances in HCO.[27−30,34,35] Very recently, Whittier and Light applied this approach to HCO for total angular momentum states $J = 0$, 1, and 3;[36] however, they used a novel, hybrid L^2-scattering approach termed the artificial boundary inhomogeneity method[37] to calculate the **S** and **Q** matrices.

One of the highlights of the earliest scattering calculations on H + CO was the marked change in the rotational state-to-state transition probabilities $P_{j\rightarrow j'}(E)$ at total energies on and off-resonance. At low collision energies and off resonance the rotational state-to-state transition probability, for example, $P_{0\rightarrow j'}(E)$, showed a marked propensity for homonuclear scattering (i.e., $P_{0\rightarrow j'}(E)$ was small for j' odd and large for j' even). (This interesting propensity was first seen and nicely explained in semiclassical calculations of He−CO scattering by McCurdy and Miller.[38]) However, at a slightly different collision energy, corresponding to a resonance, this propensity completely disappeared. This behavior, illustrated in Figure 1, was easily understood on the basis of an examination of the Legendre components of the potential. At short range, in the region of the HCO well, both even and odd components are large; however, at long range, the even components are much larger than the odd components. Off resonance, the scattering is dominated by the long-range part of the potential, whereas on resonance, the short-range part (the HCO well) dominates the dynamics. This interesting theoretical prediction has yet to be verified experimentally

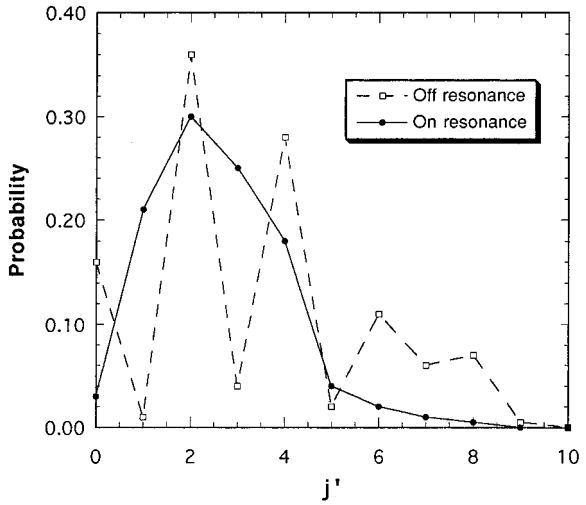

Figure 1. CO rotational distribution for H + CO scattering at a collision energy of 1664.6404 cm^{-1} (on resonance) and 1664.6448 cm^{-1} (off resonance). The zero of energy is H + CO(r_e).

The conventional scattering approach mentioned above does require an energy-by-energy search for resonances. However, this approach can be guided by the L^2 stabilization method which provides the approximate positions of resonances[39,40] The basic idea in this method is to vary a parameter of an L^2 basis, and then to plot the eigenvalues of the Hamiltonian as a function of this parameter. Resonances are identified as (unbound) eigenvalues that are stable with respect to variation of the parameter. This procedure was applied successfully to HCO by Gazdy et al.[41] Recently, an important extension of the real L^2 stabilization method has been made by Mandelshtam et al. to also obtain resonance widths.[42,43]

Complex L^2 methods can be used to obtain resonance positions and widths. That such an approach should exist seems very reasonable given that a set of isolated resonances form a spectrum with discrete *complex* energies, cf. eq 2. The earliest method of this type was based on complex scaling.[44] In this method the dissociation coordinate(s) is rotated into the complex plane, causing the kinetic energy operator and potential to become complex. A variant of this method (termed "external scaling") in which the coordinate rotation is done only for values of dissociation coordinate in the near asymptotic region has recently been applied successfully to nonrotating HCO.[45]

An alternative to complex scaling is the use of a negative imaginary absorbing potential.[46−48] In this approach the Hamiltonian is made complex by the addition of the negative imaginary potential, i.e.,

$$H_c = H - iU \quad (4)$$

where H is the real Hamiltonian, and U has the property that it vanishes, or is negligible, in the interaction region. This approach has been used to obtain resonance energies (positions and widths) for HCO. Since there is only a single continuum, corresponding to H + CO, the negative imaginary potential was taken to be a function of the distance of H to the center of mass

of CO, denoted R. In our calculations, two types of absorbing potentials were used[49−52] (i.e., a quadratic power law potential given by

$$U = 0, \quad R \le R_{\min} \qquad \text{and} \qquad R \ge R_{\max}$$

$$U = \lambda\left(\frac{R - R_{\min}}{R_{\max} - R_{\min}}\right)^2 \qquad R_{\min} \le R \le R_{\max} \qquad (5a)$$

and the Woods−Saxon potential, which is given by

$$U = \frac{2\lambda}{1 + \exp[\beta(R_{\max} - R)]} \qquad (5b)$$

In both cases the basis (or grid points) in R must extend to $R = R_{\max}$. Operationally, the complex eigenvalues are calculated as the parameters λ and β are varied, and in the case of resonances, stability with respect to these parameters is monitored. In our implementation, the real eigenfunctions of H were calculated first by an efficient truncation/recoupling method,[53] and then the multiple complex diagonalizations were done very efficiently using the real L^2 eigenfunctions of H.

Absorbing potentials have also been used in time-dependent calculations of HCO resonances,[54,55] and also in novel time-independent calculations,[56] using an extension of filter diagonalization.[57] All of these calculations were done for zero total angular momentum, $J = 0$, except for one[49] in which the even parity $J = 1$ state was also considered. Very recently, a number of papers have appeared reporting resonance energies for $J > 0$. These will be discussed in the next subsection, where the effect of rotation on resonances is presented.

All of the calculations noted above were done using the RLBH[31] Legendre polynomial representation of the ab initio BBH surface,[32] or with a modification of that surface, which was made to improve agreement with experiments on the bound states of HCO;[58,59] the modified surface is denoted RLBH-M. A newer potential energy surface has been developed by Werner et al.[60] Several modifications of this surface were made by using coordinate scaling[58,59] to improve agreement with new experiments on the bound states and resonance positions. This surface, denoted WKS-II, has been used in calculations of resonances of HCO and DCO.[61−63] The calculations of Keller et al.[61−63] were done using a scattering method (i.e., a logarthmic derivative version of the Kohn method). In this approach the experimental spectrum was directly simulated by computing the Franck−Condon factors of the excited bound vibronic state wavefunction with the bound, quasibound, and continuum states of HCO in the ground electronic state. This surface has also been used in recent extensive wavepacket calculations by Yang and Gray.[64]

It is also important to note that complex absorbing potentials are used in the entire range of time-dependent and time-independent dynamics calculations,[65] and are not restricted to the calculation of resonances. As one example, consider the photodissociation (or photodetachment) cross section out of the initial molecular bound state Φ_i. This cross section is proportional to $\langle\Phi_i|ImG^+(E)|\Phi_i\rangle$ where $G^+(E)$ is the outgoing Green's function, which can be evaluated using negative imaginary potentials.[66−68] In our work, we used the spectral representation of the outgoing Green's function

$$G^+(E) = \sum_m |\Psi_m\rangle \frac{1}{(E - E_m + i\Gamma_m/2)} \langle\Psi_m| \qquad (6)$$

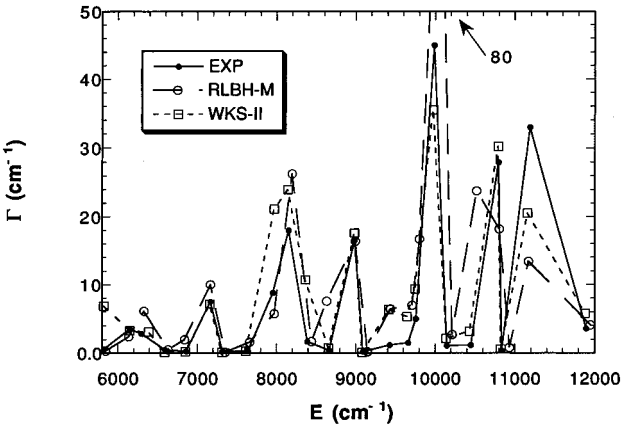

Figure 2. Comparison of calculated energies and widths of nonrotating HCO using the RLBH-M surface and the WKS-II surface with experiment for the first twenty-three experimentally observed. The zero of energy is the HCO zero-point energy. EXP is from ref 80, calculations using RLBH-M from ref 49, and those using WKS-II from ref 61.

where the $\langle\Psi_m|$ are the complex eigenfunctions of H − iU, and $E_m - i\Gamma_m/2$ are the corresponding complex eigenvalues, in calculations of photodissociation and photodetachment cross sections.[69,70]

To conclude this section on methods, we note that not all methods to calculate resonances have been reviewed here. I refer the reader to the excellent and broadly based, (if somewhat dated) edited volume on resonances in electron−molecule, van der Waals complexes, and reactive scattering calculations,[71] and in particular the chapter by Garrett et al.[72] in that volume.

Comparisons with Experiment. There have been many experiments on the bound states and resonances of HCO, so much so that it qualifies as one of the most thoroughly studied triatomic molecules. Early experiments reporting energies of excited vibrational states are those Milligan and Jacox,[73] Dixon,[74] Murray et al.,[75] Rumbles et al.,[76] and Sappey and Crosley.[77] In some of these experiments resonances were inferred; however, none had sufficient resolution to report resonance widths.

Precise measurements of the bound states and many resonances of HCO have been reported by several groups,[78−80] using stimulated emission pumping from the HCO B-state. Extensive comparisons with theory have been done using the RLBH-M and WKS-II potentials.

A sample of the comparisons between theory and experiment is shown in Figures 2 and 3. In Figure 2 calculated and experimental widths are plotted against the resonance energy for the first 23 experimental resonances. As seen, there is good qualitative and semi-quantitative agreement between theory and experiment. A comparison betweeen theory and experiment for a selected set of higher energy resonances is shown in Figure 3. As seen, there is fairly good agreement between theory and experiment, although room for improvement remains. The calculations using the WKS-II surface are in better quantitative agreement with the experiments of Rohlfing and co-workers than those using the older RLBH-M surface.

In general, the widths follow the pattern $\Gamma_{CH} > \Gamma_{bend} > \Gamma_{CO}$, where the subscript indicates the mode excited. This pattern is physically reasonable since excitation of the CH-stretch is essentially equivalent to excitation of the dissociation coordinate. Excitation of the CO-stretch is least effective in promoting dissociation, as expected since the CO-stretch is present in both HCO and the CO product, and hence it is a "spectator" mode.

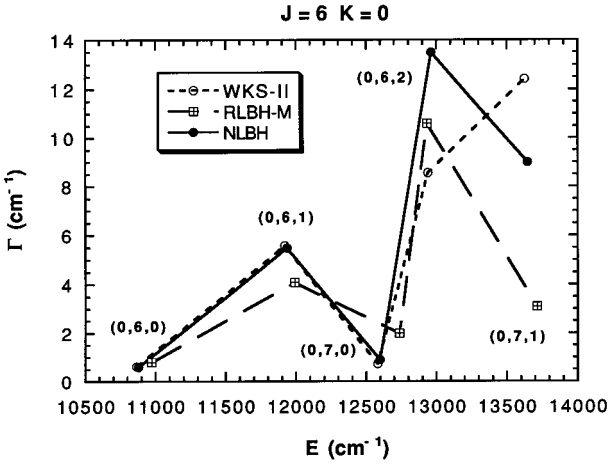

Figure 3. Comparison of calculated and experimental energies and widths of HCO resonances for $J = 6$, $K = 0$. Experiment (NLBH) is from ref 79, calculations using RLBH-M from ref 51, and calculations using WKS-II from ref 64. The first number is the CH-stretch quantum number, the second is the CO-stretch quantum number, and the third is the HCO bend quantum number.

Effect of Rotation on Resonances. Most calculations of resonances have been done for zero total angular momentum. This is understandable given that the computational effort of an exact calculation grows substantially as J increases. However, calculations of resonances HCO for J greater than zero have appeared very recently.[36,49,51,63,64,81] We reported the first exact calculation of resonances for the even-parity component of the $J = 1$ state.[49] The shifts in resonance energies relative to the $J = 0$ ones were interpreted by treating HCO as a symmetric prolate top, with standard rotation constants that depend on the resonance state. However, there did not appear to be an obvious way to interpret the changes in the widths for $J = 1$ relative to the $J = 0$ widths.

Recently, we reported a fairly extensive study of the effect of rotation on resonances in HCO using an approximate treatment of rotation that we have termed the adiabatic rotation approximation.[51] In that approximation the Hamiltonian is given by

$$H^J = H^{J=0} + E^J(Q) \tag{7}$$

where $H^{J=0}$ is the full Hamiltonian for $J = 0$ (which contains a negative imaginary, absorbing potential in our applications), and $E^J(Q)$ is the adiabatic rotational energy for the nuclear configuration denoted by Q, the collection of $3N - 6$ internal coordinates. In general, this energy is obtained by diagonalization of the inertia tensor and solution of the usual Schrödinger equation for the rotational energy eigenvalues. The procedure simplifies for symmetric tops, where the body-fixed projection quantum of J, denoted K, is also a good quantum number. In this case the rotational energy is given by the usual symmetric top expression, and for a prolate top

$$H^{J,K} = H^{J=0} + \bar{B}J(J+1) + (A - \bar{B})K^2 \tag{8}$$

where $\bar{B}$ and A are the coordinate-dependent rotation "constants" in the principal axis system. (As usual, $\bar{B}$ is the average of the B and C rotation constants.) This simplified, but very useful form of the adiabatic rotation Hamiltonian had been used by us in approximate quantum reactive scattering calculations,[82] and 20 years ago it was suggested by McCurdy and Miller in the context of a semiclassical Hamiltonian.[83] They referred to eq 8 as the principal axis/helicity-conserving approximation. Recently, Miller and co-workers applied this Hamiltonian with very good success to the direct calculation of rate constants.[84−86]

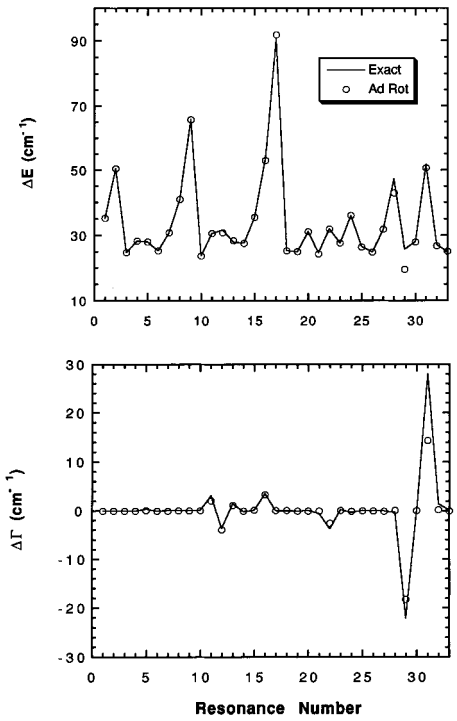

Figure 4. Comparison of exact (−) and adiabatic rotation (○) resonance energy shifts ΔE and widths ΔΓ relative to $J = 0$ results for $J = K = 1$.

The application of the adiabatic rotation approximation to resonances was first tested against our previous exact calculations for $J = 1$.[51] A comparison of the adiabatic rotation and exact *shifts* in resonance energies ΔE and widths $\Delta\Gamma$ relative to the corresponding $J = 0$ energies and width are given in Figure 4. As seen, there is very good agreement with the exact results, even though there are substantial variations in both ΔE and $\Delta\Gamma$. Note that while ΔE is always positive, $\Delta\Gamma$ is positive, negative, and also approximately zero.

Clearly, the shifts in the positions and widths with J and K depend sensitively on the resonance state. Nevertheless, we showed that the shifts in resonance positions ΔE could be fit reasonably well using the standard expression for rotational energies of a symmetric top given in eq 8. However, the value of the rotation constants $\bar{B}$ and A depend on the particular resonance state. This result is shown in Figure 5 where $\bar{B}$ and $A - \bar{B}$ are plotted for the bound and resonance states of HCO for three values of J, and $K = 1$. As seen, these "constants", although highly state-dependent, are nearly independent of J. Also shown in that figure are the rotation constants for the HCO saddle point and HCO minimum. These are true constants, and as seen the ones for the minimum are in better average agreement with the exact, fluctuating ones than are the rotation constants of the HCO dissociation saddle point. This result has significance for the validity of the J-shifting approximation,[87−89] which we discuss next.

In the J-shifting approximation,[87−89] which was introduced for reactions that proceed via direct dynamics over a single transition state, the state-to-state (i→f) transition probability $P^{JK}_{i\to f}$ is related to the one for zero total angular momentum as follows:

$$P^{JK}_{i\to f}(E) \approx P^{J=0}_{i\to f}(E - E^{\ddagger}_{JK}) \tag{9}$$

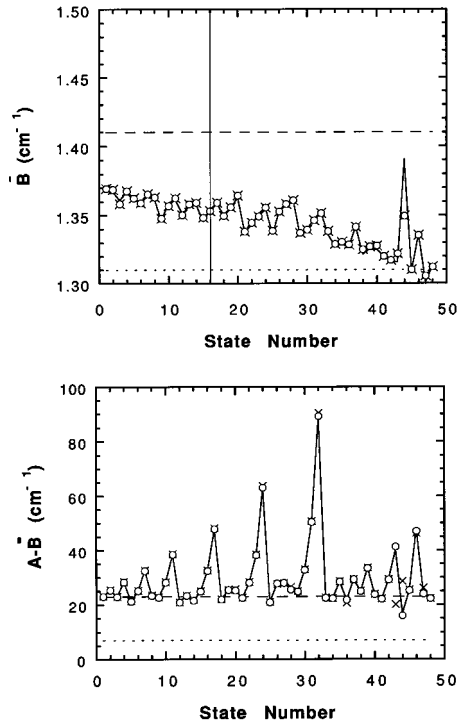

Figure 5. Comparison of the $\bar{B}$-rotation and $A-\bar{B}$-rotation constants for $J = 1$ (−), $J = 6$ (×), and $J = 20$ (○). States 1−16 are bound states and state numbers above 16 are resonances. The $\bar{B}$-constant and the $A-\bar{B}$ constant corresponding to the HCO minimum (long dash) and saddle point (short dash) are also given.

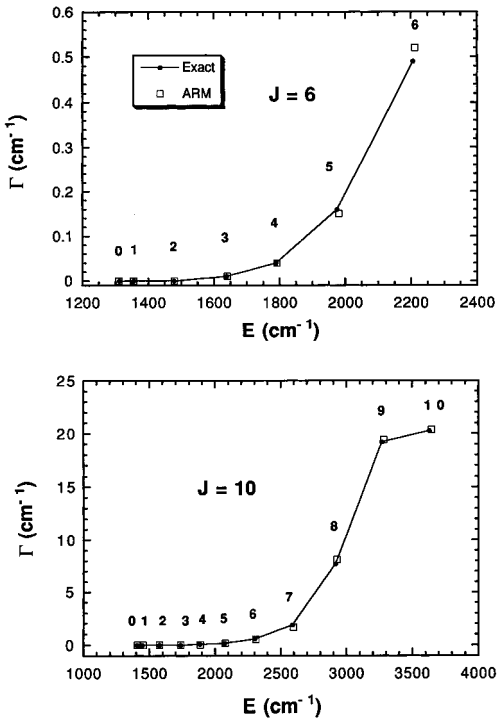

Figure 6. Comparison of exact and approximate, adiabatic rotation method (ARM), resonance energies and widths of the HCO resonance (0,0,5) for $J = 6$ and 10. The number near each data point is the value of K. Results are from ref 88.

where E is the total energy, and $E^{\ddagger}_{JK}$ is the rotational energy of the transition state. (For a linear transition state $E^{\ddagger}_{JK}$ depends only on J.) The same approximation can be made to the so-called cumulative reaction probability $N^{JK}(E)$, which is the sum of $P^{JK}_{i\to f}(E)$ over i and f. Thus, the simple J-shifting approximation for the cumulative reaction probability is

$$N^{JK}(E) \approx N^{J=0}(E - E^{\ddagger}_{JK}) \tag{10}$$

(Note that this approximation follows immediately from the adiabatic rotation approximation by replacing $E^J(Q)$ by the constant $E^{\ddagger}_{JK}$.)

The J-shifting approximation has been applied to reactions that proceed mainly via complex formation (i.e., $H + O_2$,[3,12,86,90] $OH + CO$,[21,23,91] and $H + CO$).[52] These systems all have wells, in addition to transition states, that cause pronounced resonance structure in the transition probabilities. Thus, the choice of nuclear configuration at which to evaluate $E^{\ddagger}_{JK}$ is not as obvious as in the case of direct reaction. The two obvious choices, the saddle point and the complex geometry, can give thermal rate constants that differ by as much as factors of 1.8. As noted above, we examined these two choices for the rotation constants and concluded for HCO that the rotation constants of the HCO complex were on average more accurate than those of the HCO dissociation saddle point. Another test of J-shifting at the level of the recombination rate constant will be reviewed below.

The effect of rotation on resonances in HCO has also been examined very recently using exact calculations by Whittier and Light,[36] Keller and Schinke,[63] and Yang and Gray,[64] who also tested the adiabatic rotation approximation and found it to be in good agreement with their exact calculations. A comparison of their exact and adiabatic rotation approximation widths for $J = 6$ and $J = 10$ is shown in Figure 6, where very good agreement is seen. Note that the widths of this particular resonance increases nonlinearly with K over the entire range of K.

The qualitative behavior of the widths with K shown in Figure 6 and also in Figure 4 can be understood from simple perturbation theory.[81] If we consider $H^{J=0}$ as the zeroth-order Hamiltonian $E^J(Q)$ as the perturbation, then to first order, the shift in the $J = 0$ complex resonance energies is given by the usual expression, $\langle\chi^{(0)}_n|E^J(Q)|\chi^{(0)}_n\rangle$, where $\chi^{(0)}_n$ is the complex eigenfunction of $H^{J=0}$ for the nth resonance. This complex energy shift, denoted $\Delta\epsilon^{(J)}_n$, is given by

$$\Delta\epsilon^{(J)}_n = \Delta E^{(J)}_n - \frac{i\Delta\Gamma^{(J)}_n}{2} \tag{11}$$

where $\Delta E^{(J)}_n$ and $\Delta\Gamma^{(J)}_n$ are the shifts in the position and width of the resonance.

For a prolate symmetric top, E^J is given by the usual expression, and thus

$$\Delta\epsilon^{(J,K)}_n = \langle\chi^{(0)}_n|\bar{B}|\chi^{(0)}_n\rangle J(J+1) + \langle\chi^{(0)}_n|A-\bar{B}|\chi^{(0)}_n\rangle K^2 \tag{12}$$

If we write $\chi^{(0)}_n$ in terms of its real and imaginary components,

$$\chi^{(0)}_n = \phi^{(0)}_n + i\pi^{(0)}_n \tag{13}$$

then we have

$$\Delta E^{(1)}_n = \bar{B}^{(0)}_n J(J+1) + (A^{(0)}_n - \bar{B}^{(0)}_n)K^2$$

$$\frac{-\Delta\Gamma^{(1)}_n}{4} = \beta^{(0)}_n J(J+1) + (\alpha^{(0)}_n - \bar{\beta}^{(0)}_n)K^2 \tag{14}$$

where

$$\bar{\beta}_n^{(0)} \equiv \langle \phi_n^{(0)} | \bar{B} | \phi_n^{(0)} \rangle - \langle \pi_n^{(0)} | \bar{B} | \pi_n^{(0)} \rangle \quad (15a)$$

$$A_n^{(0)} \equiv \langle \phi_n^{(0)} | A | \phi_n^{(0)} \rangle - \langle \pi_n^{(0)} | A | \pi_n^{(0)} \rangle \quad (15b)$$

$$\bar{B}_n^{(0)} \equiv \langle \pi_n^{(0)} | \bar{B} | \phi_n^{(0)} \rangle \quad (16a)$$

and

$$\alpha_n^{(0)} \equiv \langle \pi_n^{(0)} | A | \phi_n^{(0)} \rangle \quad (16b)$$

Thus, to first order, the shifts in both the positions and widths scale with J and K according to the symmetric top expression. For resonances, the real part of $\chi_n^{(0)}$ is generally much larger than the imaginary part, and so, in general, $\bar{B}_n^{(0)}$ and $A_n^{(0)}$ are positive. Thus the shifts in the resonance positions are positive, as expected. However, the shifts in the widths may be positive, zero, or negative, because the constants $\bar{B}_n^{(0)}$ and $\alpha_n^{(0)}$ may be of any sign or approximately zero. (For bound states the energies and zeroth-order wave functions are real and so the imaginary part of $\Delta\epsilon_n^{(J,K)}$ is zero.)

Perturbation theory thus provides as least a qualitative framework to understand the behavior of the shifts in positions and widths of resonances with respect to overall rotation. Of course, the validity of this framework depends on the validity of first-order perturbation theory.

We tested the accuracy of first-order perturbation theory and found good accuracy for shifts in widths less than about 10 cm^{-1}.[81] For significantly larger shifts, the accuracy of perturbation theory decreases, as expected. The results in Figure 6 confirm this indirectly. As seen, the width shows a nearly quadratic dependence on K, as predicted from perturbation theory, except for $K = 10$, for which the width is large, and where perturbation theory is evidently breaking down.

Finally, it is worth noting that another version of J-shifting results if the rigorous pertubation expression $\langle \chi_n^{(0)} | E^J(Q) | \chi_n^{(0)} \rangle$ is approximated by $E^J(\langle Q \rangle)$.

Resonances and Recombination/Dissociation. Resonances play an important role in recombination/dissociation reactions

$$A + B + M \rightleftharpoons AB + M$$

This can be seen even in the simple Lindemann mechanism in which the energized AB complex is treated in steady state and assumed to be stabilized in every collision with M. That mechanism leads to the well-known expression for the recombination rate constant

$$k_r = \frac{1}{Q_{react}} \sum_i \exp(-\beta E_i) \omega k_i / (\omega + k_i) \quad (17)$$

where k_i are the unimolecular decay rates, which in the isolated resonance limit are given by $\Gamma_i/\hbar$, where Γ_i is the width of the ith quasibound, resonance state, ω is the collision frequency, and Q_{react} is the partition function of the reactants A and B. In the quasicontinuum limit, k_r is given by

$$k_r = \frac{1}{Q_{react}} \int dE \exp(-\beta E) \rho(E) \frac{\omega k(E)}{\omega + k(E)} \quad (18)$$

where $\rho(E)$ is the density of states, and $k(E)$ is the microcanonical rate of decay (typically given by RRKM theory).

In the low pressure limit, defined by $\omega \ll k_i$, we have

$$k_r = Q_{react}(T)^{-1} \sum_i \exp(-\beta E_i) \omega = [Q_{comp}(T)/Q_{react}(T)] \omega \quad (19)$$

where Q_{comp} is the partition function of the collision complex.

There have been several quantum dynamical formulations of recombination reactions, based on the Lindemann mechanism and with the strong collision assumption. Some time ago, I proposed an extension of Smith's theory of atom−atom recombination,[92] to molecular recombination.[93] In this approach, Q_{comp} of eq 19 is given by

$$Q_{comp} = \int dE \exp(-\beta E) Tr\mathbf{Q}(E)/h \quad (20)$$

where $\mathbf{Q}(E)$ is the Smith collision lifetime matrix, eq 1, which is obtained from the full multichannel scattering matrix for the A + B scattering system.

This definition of Q_{comp} suffers from the possibility of negative values because Tr$\mathbf{Q}$ can be negative at energies where resonances do not form. At resonance energies, Tr$\mathbf{Q}$ is large and positive. This formulation of recombination was used recently by Kendrick and Pack in an application to $H + O_2$.[8,9] They compared Q_{comp} using eq 20 directly, with two variants. In one only the positive part of Tr$\mathbf{Q}$ was used, and in the other the positive part of Tr$\mathbf{Q}$ was fit to a Lorentzian. They found 15−24% differences in Q_{comp} using these three approaches, over the temperature range 100 to 600 K.

Recently, Miller proposed another quantum approach to obtain the recombination rate constant (still within the strong collision assumption).[94] Miller defined the complex region using a dividing surface, which typically would be at the dissociation saddle point or variational transition state. Within this region the complex can be stabilized with a classical probability

$$P = 1 - \exp(-\omega\tau) \quad (21)$$

where τ is the lifetime of the complex and ω is the collision frequency. This is essentially a classical picture; the generalization to quantum theory made by Miller was done by using the quantum flux−flux correlation function $C(t)$,[95] evaluated at the dividing surface, with the result[94]

$$k_r = \frac{1}{Q_{react}} \int dt \exp(-\omega t) C_f(t). \quad (22)$$

Miller has shown how his formulation reduces to the Lindemann theory, eq 17, in the limit of a set of dense, but isolated resonances.

We applied Miller's theory to recombination in H + CO;[52] however, our calculations were explicitly done only for zero total angular momentum, and the J-shifting approximation was applied to obtain the full rate constant. Making this approximation yields the following expression for $k_r(T)$:

$$k_r(T) = Q_{rot}^{*(\ddagger)}(T) k_r^{J=0}(T) \quad (23)$$

where $Q_{rot}^{*(\ddagger)}$ is the rotational partition function of the complex (or transition state) and $k_r^{J=0}(T)$ is the recombination rate constant for zero total angular momentum. As noted above, the choice of configuration to evaluate the rotation constants is not obvious for a radical−radical system. We used the rotation constants of the stable HCO to evaluate Q_{rot}^*. The other obvious choice, the recombination saddle point dividing surface, yielded a partition function 1.8 times Q_{rot}^*.

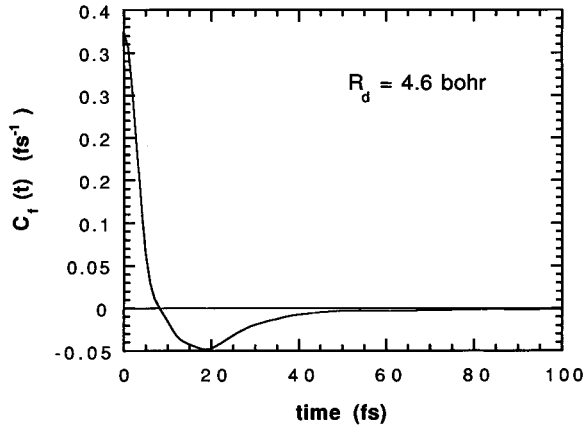

Figure 7. Flux-flux correlation function for H + CO at 1000 K evaluated at a dividing surface at the H + CO recombination saddle point.

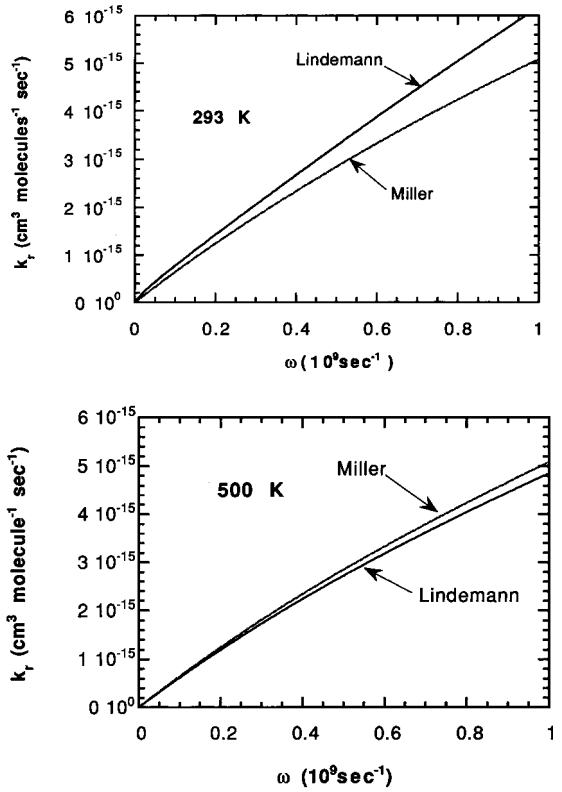

Figure 8. H + CO recombination rate constant as a function of collision frequency ω from Miller's new theory and the Lindemann theory for two temperatures indicated.

The *J*-shifting approximation also been used by Mandelshtam et al. in their recent calculation of the recombination rate for H + O_2,[12] and also by Germann and Miller in their calculations of recombination and reaction in H + O_2.[90] In both cases Q^*_{rot} of the complex was used. (Below we present a simple test of *J*-shifting for H+CO recombination.)

The $J = 0$ correlation function for H + CO is given in Figure 7 for $T = 1000$ K and for a dividing surface at the dissociation saddle point. The negative part corresponds to recrossing, outgoing flux. As seen, the flux leaves the region of the complex between 5 and 10 fs. Figure 8 shows the corresponding k_r at 293 and 500 K along with the approximate results from the Lindemann mechanism. The differences between the Lindemann and Miller theories are mainly due to the contribution from nonresonance scattering states in Miller's theory.

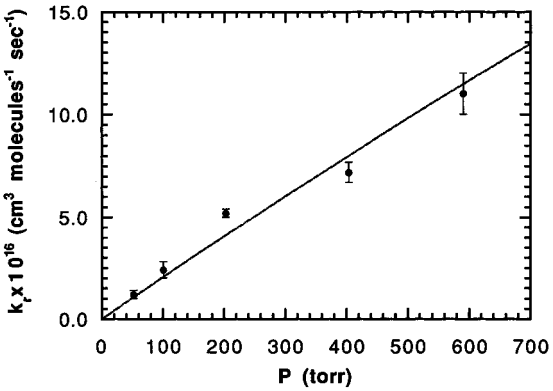

Figure 9. Comparison of experimental and calculated recombination rate constant for H + CO.

Comparison with Experiment. In order to make comparison of our results with experiment at room temperature, with Ar as the buffer gas,[96] we needed to convert the collision frequency ω to the pressure, which is the experimental independent variable. We used the simplest kinetic expression, i.e.,

$$\omega = \sigma v \frac{P}{RT} = CP \tag{24}$$

where σ is the (unknown) average cross section for the stabilization reaction, and where v is the average relative speed between Ar and metastable HCO. To determine the constant *C* we did a least-squares fit of experimental data. Then at one value of the pressure we equated the calculated rate constant to the experimental fit to determine the constant *C*. The rate constant from Miller's theory, using this calibration at one pressure, is plotted in Figure 9 as a solid line, along with the experimental data. As seen, the pressure dependence of the experimental rate constant is well reproduced by the calculations.

A Simple Test of *J*-Shifting. As already noted, *J*-shifting has been used in calculations of H + CO and H + O_2 recombination; in both cases rotation constants of complex were used. Based on the appraisal of *J*-shifting for HCO resonances given above, the expectation is that using the rotation constants of the complex would be more realistic than using those of H−CO saddle point. However, we did a direct test for H + CO recombination using the simple Lindemann equation, eq 17 to perform the test.[97] Rewriting that equation to display the summation of rotational quantum numbers explicitly, we have

$$k_r = \frac{1}{Q_{react}} \sum_{J=0}^{\infty} (2J+1) \sum_{K=-J}^{J} \sum_{i} \exp(-E_i^{J,K}/k_B T) k_i^{J,K} \omega / (k_i^{J,K} + \omega) \tag{25}$$

where the resonance energies and widths depend on *J* and *K*.

As already noted, the resonance energies for HCO could be accurately represented by the symmetric-top expression

$$E_i^{J,K} = E_i^{J=K=0} + \bar{B}_i J(J+1) + (A_i - \bar{B}_i) K^2 \tag{26}$$

where the state-dependent rotation "constants" are determined by fitting the calculated shifts in resonance energies to the symmetric top energy expression for several values of *J* and *K*. As seen in Figure 5 these constants vary considerably with the resonance state; however, in all cases are the constants nearly independent of *J* and *K*. (That the *J* and *K*-dependence of resonance energies can be represented by eq 26 is significant,

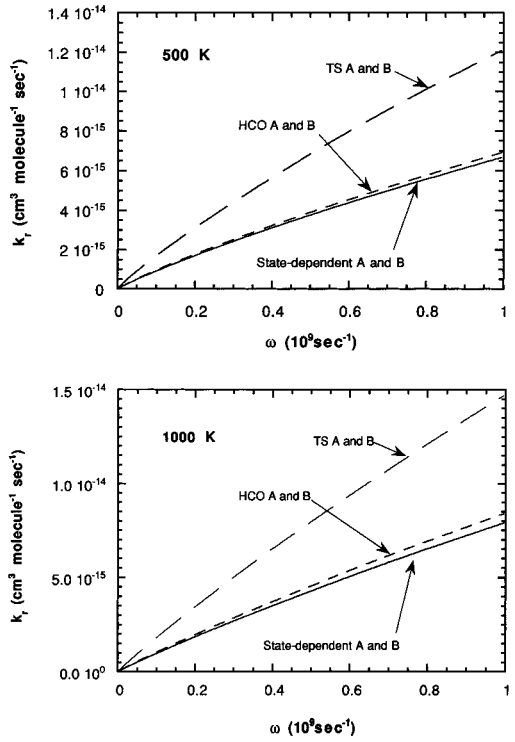

Figure 10. Recombination rate constant for H + CO using accurate resonance energies (solid line) and J-shifting approximation using rotation constants at the HCO minimum (short dash) and at the H−CO saddle point (long dash) for $T = 500$ and 1000 K.

and that expression may form the basis of the next generation of a *J*-shifting model.)

The *J*-shifting approximation to this expression is obtained by using state-independent rotation constants. For HCO at equilibrium, $\bar{B}$ equals 1.40 cm^{-1} and $A - \bar{B}$ equals 23.91 cm^{-1}. The corresponding values for $\bar{B}$ and $A - \bar{B}$ at the H−CO saddle point are 1.31 and 7.0 cm^{-1}. Thus, the HCO minimum and saddle-point values of $\bar{B}$ are quite similar but the values of *A* are quite different.

The recombination rate constant was evaluated using the full expression, eq 25, and in addition we used the $J = 0$ widths instead of the *J* and *K* dependent widths. This simplification was adequate for our purposes for two reasons. As seen in Figure 4, the *J* and *K* dependence of the shifts in the widths fluctuate about equally positively and negatively relative to the $J = 0$ widths, and so using the $J = 0$ widths is reasonable in averaged sense. Second, as noted already, the widths cancel out of the expression for k_r in the fall-off region, which is where we focused our attention. The recombination rate constant based on *J*-shifting simply uses a fixed set of rotation constants in eq 25. Since the rotation constants in J-shifting are independent of the particular resonance, the sums over *J* and *K* can be done independently to obtain the simple expression given by eq 23 above, where in the test $Q_{rot}^{*(\ddagger)}$ is the rotational partition function evaluated at the complex geometry (*) or the transition state (‡).

The results are shown in Figure 10, where the recombination rate constant based on the state-dependent rotation constants, the benchmark result, is shown along with the *J*-shifting approximation for two choices of the *A* and $\bar{B}$ constants. As seen, the choice of rotation constants corresponding to the HCO minimum gives a result that is quite close to the benchmark result. The recombination rate constant using the rotation constants corresponding to the H-CO saddle point are much larger than the correct one. This follows mainly from the small value of the *A* constant at the saddle point, which leads to a significant overestimate of the density of resonances. Thus, for this example we conclude that using the rotation constants of the HCO complex is more accurate than using rotation constants of the saddle point. (Very recently, Miller and co-workers reported that using rotation constants of the saddle point is quite accurate for the rate constant of the OH + O reaction.[86])

Beyond the Strong Collision Assumption. The strong collision assumption of the Lindemann mechanism is clearly an oversimplification. A more rigorous approach to recombination would treat the entire event as a scattering process. This would be a prohibitively demanding calculation if done exactly. Thus, we have introduced several approximations in doing such a calculation in which Ar is the collision partner M.[98] First, we treated the vibrations in a fully coupled fashion but the HCO rotation was treated using the infinite-order-sudden approximation. This approach was implemented some time ago for atom−diatom systems,[99,100] and was tested by Green et al. for H + CO at a total energy of 1 eV.[101] They found that cross sections summed over final rotational states that were larger than 0.5 a_0^2 agreed with those obtained in the more accurate centrifugal sudden approximation to within 15% or less. This result is in accord with the general expectation that the sudden treatment of rotation should be more accurate for larger cross sections than for very small ones.

The generalization of the vibrational coupled-channel/rotational sudden approximation to polyatomic molecules was made by Clary and co-workers,[102] who termed the method VCC-IOS. Their calculations focused on low-lying vibrations, which were adequately described by the harmonic-oscillator, normal-mode approximation. Such a description is not adequate for highly excited vibrational states. For that purpose we used the general Hamiltonian based on Jacobi coordinates. However, we followed much of the methodology developed by Clary and co-workers for other aspects of the calculation.

The other approximation we used is the discretization of the continuum. This approach was suggested 20 years ago by Wolken[103] and Knapp and Diestler,[104] who applied it to a model collinear system. Recently, Nobusada et al. applied this approach to several dissociation calculations, including one using the VCC-IOS method.[105]

The VCC-IOS Hamiltonian for Ar-HCO is

$$H = H_{HCO} + T_Q + \frac{L(L+1)\hbar^2}{2\mu_{Ar,HCO}Q^2} + V_{int}(r,R,\gamma,Q;\theta,\varphi) \quad (27)$$

where H_{HCO} is the Hamiltonian for nonrotating HCO, the vector **Q** is the position vector of Ar with to the center of mass of HCO, and θ and φ are the polar angles of **Q** relative to a molecule fixed coordinate system in which the *Z*-axis is along the CO bond (which is approximately the symmetric top *A*-axis.) The internal coordinates of HCO are the usual Jacobi ones, R, the distance of H to the center-of-mass of CO, *r*, the CO internuclear distance, and γ, the angle between **R** and **r**, such that linear HCO corresponds to γ equal to zero. The interaction potential V_{int} we used was a simple sum of Lennard-Jones Ar−X potentials, where X equals H, C, and O. (This is certainly a major approximation and calculations using an ab initio-based potential are underway.)

The scattering wavefunction is given by a coupled-channel expansion in terms of the HCO vibrational wave functions, $F_n(r,R,\gamma)$, times unknown radial wave functions, $g_n^L(Q;\theta,\varphi)$, as follows:

$$\Psi^L(Q,r,R,\gamma;\theta,\varphi) = \sum_n F_n(r,R,\gamma) g_n^L(Q;\theta,\varphi) \qquad (28)$$

Inserting this expansion of the wave function into the Schrödinger equation yields the standard matrix differential equations for the radial wave functions:

$$\frac{-\hbar^2}{2\mu_{Ar,HCO}} \underset{\approx}{g}^L(Q;\theta,\varphi) + \left[\frac{L(L+1)}{2\mu Q^2} \underset{\approx}{I} + \underset{\approx}{V}(Q;\theta,\varphi) - \underset{\approx}{E}\right] \underset{\approx}{g}^L(Q;\theta,\varphi) = 0 \quad (29)$$

where $V_{n'n} = \langle F_{n'}|V_{\rm int}|F_n\rangle$, $E_{n'n} = (E - \epsilon_n)\delta_{n'n}$, and where ϵ_n are the vibrational eigenvalues and E is the total energy.

After propagating the solution matrix $\underset{\approx}{g}^L(Q;\theta,\varphi)$ to the noninteracting region, the scattering matrix $\underset{\approx}{S}^L(E;\theta,\phi)$ is obtained, and from it, the cross section for the transition from the initial state i to the final state f is given by

$$Q_{i,j}(E) = \frac{\pi}{k_i^2} \sum_{L=0} (2L+1) \langle |S_{i,f}^L(E) - \delta_{i,f}|^2 \rangle \qquad (30)$$

where $\langle |S_{i,f}^L(E)|^2 \rangle$ is the spherical average of $|S_{i,f}^L(E;\theta,\phi)|^2$. This cross section is implicitly summed over final rotational states of HCO and corresponds to the initial nonrotating state. In our implementation of this approach, we preaveraged the interaction potential over ϕ to save computer effort, and so the scattering matrix is only a function of θ.

The one set of results of this calculation that I review here are the collision-induced dissociation cross sections. These were calculated for each initial bound state to all final unbound states. To condense the information, the cross sections were summed over all final unbound states corresponding to resonances, and also separately to unbound, nonresonance states. These cross sections are plotted separately for the two largest sets of cross sections in Figure 11. Both states shown have initial excitation in the CH-stretch. As seen, the cross sections corresponding to resonances are considerably larger than the ones corresponding to excitation of non-resonance states; however, cross sections to nonresonance states are not negligible. By microscopic reversibility this implies that while recombination is dominated by resonances, direct recombination from nonresonant scattering is not negligible. Clearly the relative importance of resonances in recombination/dissociation is qualitatively governed by the density of resonances. HCO has a fairly sparse set of resonances, and even so, they dominate dissociation, because energy transfer to (and from them) is far more probable than to non-resonance scattering states. However, as recently shown by Pack and co-workers[106] for atom−atom recombination, nonresonant dissociation can dominate resonant dissociation if the spectrum of resonances is very sparse.

Next, I review our calculations on resonances in HOCO, and raise issues about reduced-dimensionality approaches to describe reactions in larger systems that are dominated by resonances.

HOCO. The reaction OH + CO → H + CO_2 is of importance in combustion and in atmospheric chemistry, and from a basic research perspective it has become an important prototype of reactions that proceed via complex formation. The reaction has been extensively studied both and theoretically and experimentally. (References to the extensive experimental literature can be found in the theoretical papers, cited below.) Theoretical interest in this reaction began with a realistic potential energy surface that was used in extensive quasiclassical trajectory calculations.[107−109]

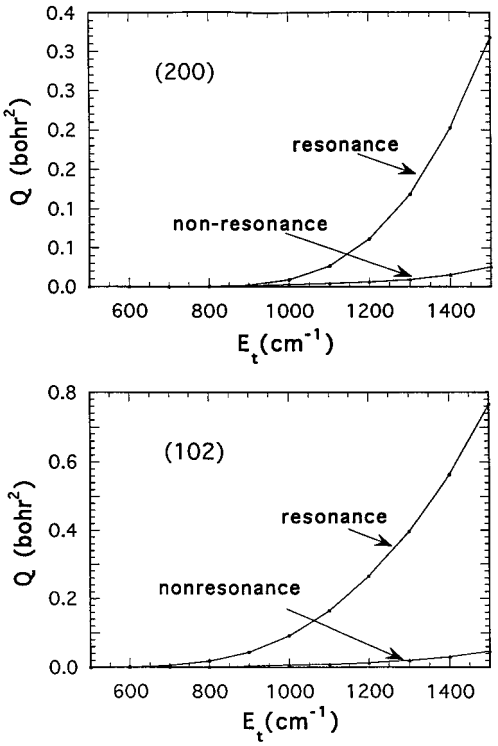

Figure 11. Collision-induced dissociation cross section for the two initial HCO states indicated. The curve labeled "resonance" is the cross section summed over all resonances. The curve labeled "nonresonance" is the cross section summed over all nonresonances.

The first quantum calculations of the reaction probability were done by Schatz and Dyke.[18] They used a two-degree-of-freedom, reduced dimensionality approach in which the nonreactive CO bond was treated as a spectator. The two active degrees of freedom were the OH bond length and the distance between the OH and CO centers of mass. The full six-degree-of-freedom (DOF) potential was minimized for fixed values of these two distances with respect to two internal angles and the spectator CO stretch. At each minimum the local zero-point energy of the two bends and CO stretch was calculated and added to the potential at the minimum.

The calculated reaction probability exhibited sharp resonant structure which was attributed to quasibound states of HOCO. Subsequently, scattering calculations on the 2-DOF reduced dimensionality potential were reported by Hernandez and Clary.[19] They also reported calculations of the resonance positions and widths, using a stabilization method recently extended developed by Mandelshtam and Taylor[42,110] to also provide resonance widths. They found generally good agreement between the stabilization results and the exact results from the scattering calculation. However, widths from the stabilization calculations were not reported for a number of the narrower resonances. We recently used a complex absorbing potential in the two arrangement channels, OH + CO and H + CO_2, and an extended L^2 basis to calculate the resonances of the 2-DOF Hamiltonian.[20] We obtained very good agreement for the positions and widths for all the resonances reported in the scattering calculations, as shown in Table 1.

There have also been limited 3-,[22] 4-,[23] and 5-DOF[24] quantum calculations of the reaction probabilities for this reaction. However, these were for a limited number of initial rotational states of OH, and so it was not possible to use standard energy-

TABLE 1: Comparison of Present Resonance Energies and Widths for HOCO with Those of Hernandez and Clary (HC) (Reference 19)

E (cm^{-1})			Γ (cm^{-1})		
present	HC-scatt	HC-stab	present	HC-scatt	HC-stab
2699.0	2698.0	2698.0	0.092	0.141	
2730.0	2729.0	2728.0	1.65	1.82	2.16
2752.2	2748.0	2754.0	0.89	1.10	
2768.3	2766.0	2769.0	0.54	0.527	
3241.3	3240.0	3241.0	0.37	0.406	
3282.6	3280.0	3281.0	1.13	1.22	1.01
3308.6	3307.0	3307.0	2.42	2.71	2.25
3762.8	3761.0	3762.0	0.63	0.745	
3815.6	3814.0	3813.0	0.25	0.252	
3864.3	3863.0	3862.0	2.44	2.49	2.42
4249.2	4246.0	4248.0	1.12	1.29	1.31
4353.4	4351.0	4352.0	0.25	0.225	
4424.5	4423.0	4422.0	4.96	4.63	4.51
4699.4	4696.0	4698.0	3.24	3.48	2.99
4882.5	4880.0	4880.0	0.29	0.291	
4977.3	4976.0	4975.0	3.74	4.43	5.98
5111.5	5107.0	5110.0	5.97	6.65	6.19
5398.5	5396.0	5396.0	1.76	2.00	2.88
5494.9	5490.0	5493.0	7.21	6.65	2.91
5528.3	5527.0	5526.0	5.71	7.49	5.48
5820.9	5816.0	5820.0	6.54	7.00	8.06
5915.6	5912.0	5914.0	0.48	0.430	
6072.2	6073.0	6071.0	15.3		
6086.5	6080.0	6090.0	1.79		
6410.5			9.59		
6611.9			11.7		
6893.2			9.99		
7352.9			9.39		

shifting approaches[86,88] to obtain an approximate, full 6-DOF cumulative reaction probability (CRP). For that reason, we used the 2-DOF scattering calculations[18,19] to obtain an approximate 6-DOF CRP. Thus, the approximate 6-DOF CRP was given by[91]

$$N(E) = \sum_J (2J+1) \sum_{K=-J}^{J} N^{J=0}(E - E_{JK}) \qquad (31)$$

where

$$N^{J=0}(E) = \sum_{n=0} N^{2-DOF}(E - E_n^{\ddagger}) \qquad (32)$$

and where $N^{2-\mathrm{DOF}}(E)$ is the 2-DOF CRP (which we obtained from previous scattering calculations[18,19]), $E_n^{\ddagger}$ are the quantized energies at the cis $H-CO_2$ transition state (using the harmonic normal mode frequencies) not explicitly included in the 2-DOF Hamiltonian, and E_{JK} are the rotational energies of HOCO, treated as a symmetric prolate top. We considered two configurations in which to obtain rotation constants for the $J(K)$-shifting, and found a factor of about 1.5 difference in the resulting rate constant, with the $H-CO_2$ transition state rate constant being about 1.5 times smaller than the rate constant using the rotation constants of HOCO. The approximate N(E) given above and using the transition state rotation constants is shown in Figure 12. As seen, it is highly structured, but on the average increasing with E, the total energy. The increase with E is due to overlapping of resonances in the 2-DOF scattering calculation.

While it is clear that the exact $N(E)$ is all that is needed to obtain the exact bimolecular rate constant, independent of whether the reaction is characterized as "direct" or "complex" (i.e., resonance-dominated), there does exist some ambiguity about the proper approximation to make to a reduced dimensionality CRP to get the best approximate full dimensional CRP. That is, should $N(E)$ be approximated by transition state theory appropriate for a direct reaction or by statistical theory, which is appropriate for a complex-forming reaction? The energy-shifting approximation used above assumes that the dynamical bottleneck in going from 2-DOF to 6-DOF is at the exit transition state. However, other choices are possible, and the "correct" choice is still an open question. A detailed discussion of this important point can be found in papers by Dzegilenko and Bowman[91] and Wang et al.[111]

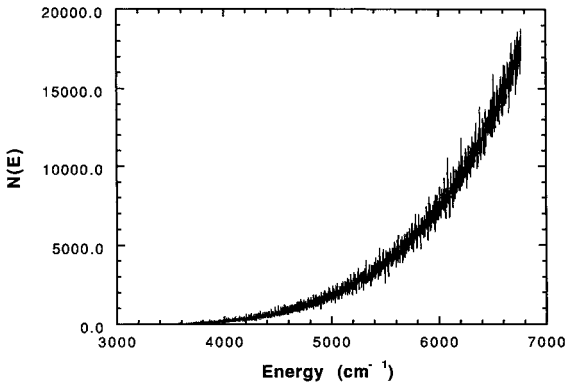

Figure 12. Cumulative reaction probablity for $OH + CO \rightarrow H + CO_2$.

Another important issue is the treatment of the CO spectator mode in the OH + CO reaction. As noted above, the CO-stretch was decoupled in all quantum scattering calculations performed to date. The possible justification for this is that this bond is nonreactive, meaning that it is present both in the reactants and in the products. Thus, one can expect that it does not actively exchange energy with the other five modes and could be treated adiabatically or simply averaged over. However, there are two nagging counterpoints to this argument. The most evident one is that while the CO-stretch is a "normal mode" for the CO molecule, it is not for CO_2. (The difference between the symmetric and antisymmetric stretches in CO_2 is slightly more than 1000 cm^{-1} indicating that CO_2 cannot be described, even approximately, as two uncoupled CO oscillators.) The other point is that HOCO resonances in which the CO-stretch is highly excited certainly exist. What is not known is the extent to which these resonances contribute to the CRP. Also, a related issue is whether the inclusion of the CO-stretch can be approximated by a simple energy-shift approximation, as was done in eq 31. Note this energy shift, when applied to resonances, simply means that 3-DOF resonances are approximated by the set of 2-DOF resonances shifted by the addition of CO vibrational energies.

To begin an examination of the role played by the CO stretch we performed 3-DOF complex L^2 calculations of 218 resonances with the CO mode explicitly considered.[21] We were able to assign quantum numbers to many of these resonances, and could identify those that correspond to highly excited CO. The spectrum of these 3-DOF resonances is shown in Figure 13 along with the previous 2-DOF resonances for energies in which both OH + CO and H + CO_2 channels are open. As seen, there is a distinct set of additional resonances that stand out from the 2-DOF ones in having much smaller widths than the widths 2-DOF resonances. These narrow resonances are ones in which the CO-stretch is highly excited. We next examined the extent to which these additional resonances could be recovered using a simple CO-stretch energy shift applied to the 2-DOF resonances. (We used a simple harmonic approximation for the CO-stretch vibrational energy, and used the frequency

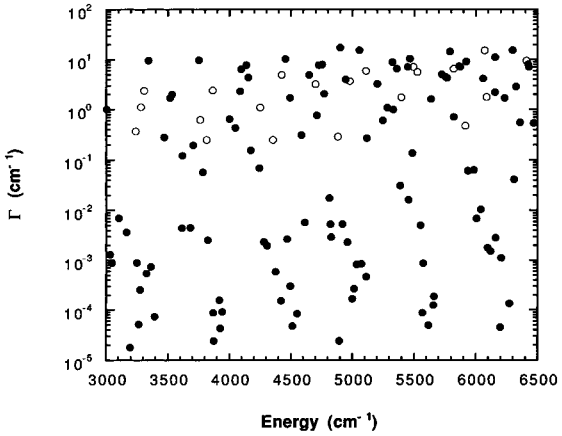

Figure 13. Three-DOF (●) and 2-DOF (○) energies and widths of nonrotating HOCO resonances.

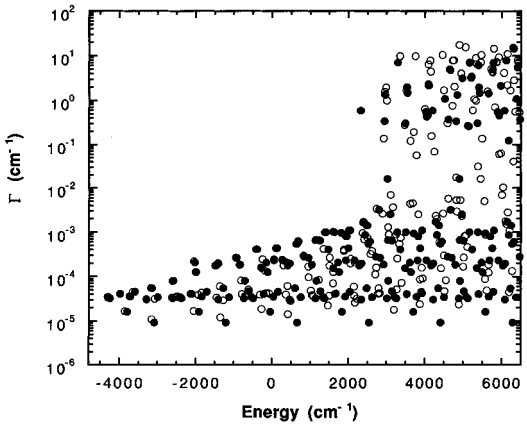

Figure 14. Three-DOF (●) and energy-shifted 2-DOF (○) energies and widths of nonrotating HOCO resonances.

of the CO-mode in HOCO, 1875 cm^{-1}.) The results are shown graphically in Figure 14 for the entire energy range spanning energies where the HOCO complex can decompose. As seen, the detailed results are at least qualitatively similar, and coarse-grained averaging shows semiquantitative agreement.[21] Note especially that the additional narrow resonances in Figure 12 for energies above 3000 cm^{-1} appear in this figure by applying the energy-shift to the 2-DOF resonances.

Thus, most of the narrow 3-DOF resonances are built on low-energy 2-DOF resonances with the addition of CO vibrational excitation. Note that the widths of the shifted 2-DOF resonances are unaffected by the CO energy-shift. There are among the dense set of 3-DOF resonances a small number of very narrow resonances that correspond to true bound states in the 2-DOF space but in three degrees of freedom are resonances due to high overtone excitation of the CO stretch. These resonances cannot be accounted for obviously by an energy-shift approximation.

Overall, the 3-DOF resonance spectrum is reasonably well approximated by the shifted 2-DOF resonances. It remains to be seen if the 3-DOF cumulative reaction probability can be well approximated by the shifted 2-DOF one.

Summary and Possible Future Directions. I reviewed methods to calculate and characterize resonances in molecular complexes, and presented extensive results, including comparisons between theory and experiment, for HCO. The effect of overall rotation on the positions and widths of resonances was also examined in detail, and several tests of the adiabatic rotation approximation, first-order perturbation theory, and *J*-shifting were presented. The importance of resonances in the Lindemann theory of dissociation/recombination reactions was described, as was an application of Miller's new theory of recombination to H + CO. The first calculations to describe dissociation of HCO in collisions with Ar using scattering theory were also reviewed. Resonances in HCO were shown to play a major, though not totally dominant role in dissociation/recombination. More calculations of this type will be useful in order to test and modify the "strong collision assumption", which is made in the Lindemann theory as well as Miller's new theory. It will also be important also to develop realistic interaction potentials for recombination dynamics.

I also reviewed reduced dimensionality models for resonances and the cumulative reaction probability for the H + CO_2 → [HOCO] → OH + CO reaction. An important issue that needs further study is how to best approximate the full dimensionality cumulative reaction probability from a reduced dimensionality calculation (i.e., whether the standard energy-shift approach continues to be apply, or whether a statistical treatment of uncoupled degrees of freedom is better). A partial study of this was reviewed by examining the role of the spectator CO-stretch in the spectrum of HOCO resonances. This was done for the three-degree-of-freedom model with those of a 2-DOF model which does not include coupling to the CO-stretch. While not all the 3-DOF resonances can be accounted for by applying simple energy-shifts to the 2-DOF spectrum, most were. This provides some evidence that simple energy-shifting may still apply to complex-forming reactions. A definitive test in which energy shifting applied to the 2-DOF cumulative reaction probability is compared to the 3-DOF cumulative reaction probability needs to be done.

Acknowledgment. I thank my co-authors and co-workers Fedor Dzegilenko, Jianxin Qi, Baiyu Pan, Desheng Wang, Bela Gazdy, Al Wagner, and Larry Harding with whom it has been a pleasure to work over a number of years. I also thank the Department of Energy for financial support, as well as the reviewers for helpful comments.

References and Notes

(1) Schatz, G. C. *J. Phys. Chem.* **1990**, *94*, 6157.
(2) Manolopoulos, D. E. *J. Chem. Soc., Faraday Trans.* **1997**, *93*, 673.
(3) Leforestier, C.; Miller, W. H. *J. Chem. Phys.* **1994**, *100*, 733.
(4) Zhang, D. H.; Zhang, J. Z. H. *J. Chem. Phys.* **1994**, *101*, 3671.
(5) Dai, J.; Zhang, J. Z. H. *J. Chem. Phys.* **1996**, *104*, 3664.
(6) Dobbyn, A. J.; Stumpf, M.; Keller, H.-M.; Hase, W. L.; Schinke, R. *J. Chem. Phys.* **1995**, *102*, 5867.
(7) Dobbyn, A. J.; Stumpf, M.; Keller, H.-M.; Schinke, R. *J. Chem. Phys.* **1996**, *104*, 8357.
(8) Kendrick, B.; Pack, R. T. *Chem. Phys. Lett.* **1995**, *235*, 291.
(9) Kendrick, B.; Pack, R. T. *J. Chem. Phys.* **1996**, *104*, 7502.
(10) Kendrick, B.; Pack, R. T. *J. Chem. Phys.* **1997**, *106*, 3519.
(11) Mandelshtam, V. A.; Grozdanov, T. P.; Taylor. *J. Chem. Phys.* **1995**, *103*, 10074.
(12) Mandelshtam, V. A.; Taylor, H. S.; Miller, W. H. *J. Chem. Phys.* **1996**, *105*, 496.
(13) Mandelshtam, V. A.; Taylor, H. S. *J. Chem. Soc., Faraday Trans.* **1997**, *93*, 847.
(14) Parker, G. A.; Laganá, A.; Crocchianti, S.; Pack, R. T. *J. Chem. Phys.* **1995**, *102*, 1238.
(15) Balint-Kurti, G. G.; Gogtas, F.; Mort, S. P.; Offer, A. R.; Laganá, A.; Gervasi, O. *J. Chem. Phys.* **1993**, *99*, 9567.
(16) Gogtas, F.; Balint-Kurti, G. G.; Offer, A. R. *J. Chem. Phys.* **1996**, *104*, 7927.
(17) Zhu, W. W., D Y.; Zhang, J Z H.; *Theoretical Chemistry Accounts* **1997**, *96*, 31.
(18) Schatz, G. C.; Dyck, J. *Chem. Phys. Lett.* **1992**, *188*, 11.
(19) Hernandez, M. I.; Clary, D. C. *J. Chem. Phys.* **1994**, *101*, 2779.
(20) Bowman, J. M.; Metropoulos, A. *J. Chem. Soc., Faraday Trans.* **1997**, *93*, 815.
(21) Dzegilenko, F. N.; Bowman, J. M. *J. Chem. Phys.* **1998**, *108*, 511.

(22) Clary, D. C.; Schatz, G. C. *J. Chem. Phys.* **1993**, *99*, 4578.
(23) Goldfield, E. M.; Gray, S. K.; Schatz, G. C. *J. Chem. Phys.* **1995**, *102*, 8807.
(24) Zhang, D. H.; Zhang, J. Z. H. *J. Chem. Phys.* **1995**, *103*, 6512.
(25) Gezelter, J. D.; Miller, W. H. *J. Chem. Phys.* **1995**, *103*, 7868.
(26) Hernandez, R., Miller, W. H., Moore, C. B., Polik, W. F. *J. Chem. Phys.* **1993**, *99*, 950.
(27) Lee, K. T.; Bowman, J. M. *J. Chem. Phys.* **1986**, *85*, 6225.
(28) Lee, K. T.; Bowman, J. M. *J. Chem. Phys.* **1987**, *86*, 215.
(29) Cho, S. W.; Wagner, A. F.; Gazdy, B.; Bowman, J. M. *J. Chem. Phys.* **1992**, *96*, 2799.
(30) Cho, S. W.; Wagner, A. F.; Gazdy, B.; Bowman, J. M. *J. Chem. Phys.* **1992**, *96*, 2812.
(31) Romanowski, H.; Lee, K.-T.; Bowman, J. M.; Harding, L. B. *J. Chem. Phys.* **1986**, *84*, 4888.
(32) Bowman, J. M.; Bittman, J. S.; Harding, L. B. *J. Chem. Phys.* **1986**, *85*, 911.
(33) Smith, F. T. *Phys. Rev.* **1960**, *118*, 349.
(34) Bowman, J. M. *Int. J. Quantum Chem., Quantum Chem. Symp* **1986**, *20*, 681.
(35) Cho, S. W.; Wagner, A. F.; Gazdy, B.; Bowman, J. M. *J. Phys. Chem.* **1991**, *95*, 9897.
(36) Whittier, G. S.; Light, J. C. *J. Chem. Phys.* **1997**, *107*, 1816.
(37) Jang, H. W.; Light, J. C. *J. Chem. Phys.* **1995**, *102*, 3262.
(38) McCurdy, C. W.; Miller, W. H. *J. Chem. Phys.* **1977**, *99*, 463.
(39) Taylor, H. S. *Adv. Chem. Phys.* **1970**, *17*, 91.
(40) Hazi, A. U.; Taylor, H. S. *Phys. Rev.* **1970**, *A1*, 1109.
(41) Gazdy, B.; Bowman, J. M.; Cho, S. W.; Wagner, A. F. *J. Chem. Phys.* **1991**, *94*, 4192.
(42) Mandelshtam, V. A.; Taylor, H. S.; Ryaboy, V.; Moiseyev. *Phys. Rev. A* **1994**, *50*, 2764.
(43) Mandelshtam, V. A.; Ravuri, T. R.; Taylor, H. S. *Phys. Rev. Lett.* **1993**, *70*, 1932.
(44) Reinhardt, W. P. *Annu. Rev. Phys. Chem.* **1982**, *33*, 223.
(45) Ryaboy, V.; Moiseyev, N. *J. Chem. Phys.* **1995**, *103*, 4061.
(46) Jolicard, G.; Leforestier, C.; Austin, E. J. *J. Chem. Phys.* **1988**, *88*, 1026.
(47) Jolicard, G.; Austin, E. *Chem. Phys. Lett.* **1985**, *121*, 106.
(48) Jolicard, G.; Austin, E. *Chem. Phys.* **1986**, *103*, 295.
(49) Wang, D.; Bowman, J. M. *Chem. Phys. Lett.* **1995**, *235*, 277.
(50) Wang, D.; Bowman, J. M. *J. Chem. Phys.* **1994**, *100*, 1021.
(51) Qi, J.; Bowman, J. M. *J. Chem. Phys.* **1996**, *105*, 9884.
(52) Qi, J.; Bowman, J. M. *J. Phys. Chem.* **1996**, *100*, 15165.
(53) Bowman, J. M.; Gazdy, B. *J. Chem. Phys.* **1991**, *94*, 454.
(54) Dixon, R. N. *J. Chem. Soc., Faraday Trans.* **1992**, *88*, 2575.
(55) Gray, S. K. *J. Chem. Phys.* **1992**, *96*, 6543.
(56) Grozdanov, T. P.; Mandelshtam, V. A.; Taylor, H. S. *J. Chem. Phys.* **1995**, *103*, 7990.
(57) Wall, M. R.; Neuhauser, D. *J. Chem. Phys.* **1995**, *102*, 8011.
(58) Bowman, J. M.; Gazdy, B. *J. Chem. Phys.* **1991**, *94*, 816.
(59) Bowman, J. M.; Gazdy, B. *Chem. Phys. Lett.* **1992**, *200*, 311.
(60) Werner, H.-J.; Bauer, C.; Rosmus, P.; Keller, H.-M.; Stumpf, M.; Schinke, R. *J. Chem. Phys.* **1995**, *102*, 3593.
(61) Keller, H.-M.; Floethmann, H.; Dobbyn, A. J.; Schinke, R.; Werner, H.-J.; Bauer, C.; Rosmus, P. *J. Chem. Phys.* **1996**, *105*, 4983.
(62) Keller, H.-m.; Stumpf, M.; Schroeder, T.; Stoeck, C.; Temps, F.; Schinke, R.; Werner, H.-J.; Bauer, C.; Rosmus, P. *J. Chem. Phys.* **1997**, *106*, 5359.
(63) Keller, H.-M.; Schinke, R. *J. Chem. Soc., Faraday Trans.* **1997**, *93*, 879.
(64) Yang, C.-Y.; Gray, S. K. *J. Chem. Phys.* **1997**, *107*, 7773.
(65) Wyatt, R. E., Zhang, J. Z. H., Eds. *Dynamics of Molecules and Chemical Reactions*; Mracel Dekker: New York, 1996.
(66) Neuhauser, D.; Baer, M. *J. Chem. Phys* **1989**, *90*, 4351.
(67) Seideman, T.; Miller, W. H. *J. Chem. Phys.* **1992**, *96*, 4412.
(68) Seideman, T. *J. Chem. Phys.* **1993**, *98*, 1989.
(69) Mayrhofer, R. C.; Bowman, J. M. *J. Chem. Phys.* **1995**, *102*, 5598.
(70) Mayrhofer, R. C.; Bowman, J. M. *J. Chem. Phys.* **1994**, *100*, 7229.
(71) Truhlar, D. G., Ed. *Resonances*; American Chemical Society: Washington, DC, 1984.
(72) Garrett, B. C.; Schwenke, D. W.; Skodje, R. T.; Thirumulai, D.; Thompson, T. C.; Truhlar, D. G. In *Resonances*; Truhlar, D. G., Ed.; ACS: Washington, DC, 1984; Chapter 20.
(73) Milligan, D. E.; Jacox, M. E. *J. Chem. Phys.* **1964**, *41*, 3032.
(74) Dixon, R. N. *Trans. Faraday Soc.* **1969**, *564*, 3141.
(75) Murray, K. K.; Miller, T. M.; Leopold, D. G.; Lineberger, W. C. *J. Chem. Phys.* **1986**, *84*, 2520.
(76) Rumbles, G.; Lee, E. K. C.; Valentini, J. J. *J. Chem. Soc., Faraday Trans.* **1990**, *86*, 3837.
(77) Sappey, A. D.; Crosley, J. *J. Chem. Phys.* **1990**, *93*, 7601.
(78) Adamson, G. W.; Zhao, Z.; Field, R. W. *J. Mol. Spectrosc.* **1993**, *160*, 11.
(79) Neyer, D. W.; Luo, X.; Burak, I.; Houston, P. L. *J. Chem. Phys.* **1995**, *102*, 1645.
(80) Tobiason, J. D.; Dunlop, J. R.; Rohlfing, E. A. *J. Chem. Phys.* **1995**, *103*, 1448.
(81) Qi, J.; Bowman, J. M. *J. Chem. Phys.* **1997**, *107*, 9960.
(82) Wang, D.; Bowman, J. M. *J. Phys. Chem.* **1994**, *98*, 7994.
(83) C. W.; Miller, W. H In *State-to-State Chemisty*; Brooks, P. R., Hayes, E. F., Eds.; American Chemical Society: Washington, DC, 1977; pp 239−242.
(84) Wang, H.; Thompson, W. H.; Miller, W. H. *J. Chem. Phys* **1997**, *107*, 7194.
(85) Thompson, W. H.; Miller, W. H. *J. Chem. Phys.* **1997**, *106*, 142.
(86) Skinnner, D. E.; Germann, T. C.; Miller, W. H. *J. Phys. Chem.* **1998**. In press.
(87) Bowman, J. M. *Adv. Chem. Phys.* **1985**, *61*, 115.
(88) Bowman, J. M. *J. Phys. Chem.* **1991**, *95*, 4960.
(89) Sun, Q.; Bowman, J. M.; Schatz, G. C.; Sharp, J. R.; Connor, J. N. L. *J. Chem. Phys* **1990**, *92*, 1677.
(90) Germann, T. C.; Miller, W. H. *J. Phys. Chem.* **1997**, *101*, 6358.
(91) Dzegilenko, F. N.; Bowman, J. M. *J. Chem. Phys.* **1996**, *105*, 2280.
(92) Smith, F. T. In *Kinetic Processes in Gases and Plasmas*; Hochstim, A. R., Ed.; Academic: New York, 1969; pp 321−380.
(93) Bowman, J. M. *J. Phys. Chem.* **1986**, *90*, 3492.
(94) Miller, W. H. *J. Phys. Chem.* **1995**, *99*, 12387.
(95) Miller, W. H.; Schwartz, S. D.; Tromp, J. W. *J. Chem. Phys.* **1983**, *79*, 4889.
(96) Ahumada, J. J.; Michael, J. V.; Osborne, D. T. *J. Chem. Phys* **1972**, *57*, 3736.
(97) Qi, J.; Bowman, J. M. *Chem. Phys. Lett.* **1997**, *276*, 371.
(98) Pan, B.; Bowman, J. M. *J. Chem. Phys.* **1995**, *103*, 9661.
(99) Schinke, R.; McGuire, P. *Chem. Phys.* **1978**, *28*, 129.
(100) Leasure, S. C.; Bowman, J. M. *J. Chem. Phys.* **1977**, *66*, 288.
(101) Green, S.; Pan, B.; Bowman, J. M. *J. Chem. Phys* **1995**, *102*, 8800.
(102) Clary, D. C. *J. Phys. Chem.* **1987**, *91*, 1718.
(103) Wolken, G. J. *J. Chem. Phys.* **1975**, *63*, 528.
(104) Knapp, E.-W.; Diestler, D. J. *J. Chem. Phys.* **1977**, *67*, 4969.
(105) Nobusada, K.; Sakimoto, K. *J. Chem. Phys.* **1997**, *206*, 9078.
(106) Pack, R. T.; Walker, R. B.; Kendrick, B. K. *Chem. Phys. Lett.* **1997**, *276*, 255.
(107) Kudla, K.; Schatz, G. C.; Wagner, A. F. *J. Chem. Phys.* **1991**, *95*, 1635.
(108) Kudla, K.; Koures, A. G.; Schatz, G. C.; Wagner, A. F. *J. Chem. Phys.* **1992**, *96*, 7465.
(109) Schatz, G. C.; Fitzcharles, M. S.; Harding, L. B. *Faraday Discuss., Chem. Soc.* **1987**, *84*, 359.
(110) Mandelshtam, V. A.; Ravuri, T. R.; Taylor, H. S. *J. Chem. Phys.* **1994**, *101*, 8792.
(111) Wang, H.; Goldfield, E. M.; Hase, W. L. *J. Chem. Soc., Faraday Trans.* **1997**, *93*, 737.